Unveiling Dynamics in EU Carbon Emissions Futures

A Comprehensive Analysis with Interlinked Financial Indices

Yucong Chen, Jayanthi Yerchuru

December 21, 2023

Abstract This study examines the dynamics in EU carbon emissions futures and offers a comprehensive analysis of both long- and short-term data. We develop a time series econometrics model to predict daily log returns of carbon emission futures. We explore long-term stochastic and volatile patterns in the dataset, providing perspectives on both the carbon market and the broader financial landscape. In addition, we reveal the intricate relationship between EU carbon emissions futures and Tesla stock prices, offering insights into their co-movement and its impacts on market dynamics.

1 Introduction

This paper aims to model and understand the dynamics of EU carbon emissions futures (CFI2Z3) from both a long-term and short-term perspective. Carbon emissions futures refer to financial contracts that allow market participants to buy or sell the right to emit a specific amount of carbon dioxide at a predetermined price on a future date [6]. Excessive emissions of carbon dioxide and other greenhouse gases put enormous pressure on the climate and the environment and are toxic to human health. This situation has intensified over the last decade. From an economic point of view, carbon emissions cause significant negative externalities for society. Using futures as a way of pricing carbon emissions can help reduce the gap of negative externalities and discourage such behavior. Currently, the European Union Emissions Trading System (EU-ETS) is the world's first major carbon market and remains the biggest one [1]. Trading of carbon allowances using a Cap and Trade system encourages power stations and industrial plants which contribute largely to emissions to use clean energy. This leads directly to the widespread interest in carbon price forecasting and the study of carbon futures' price dynamics.

EU-ETS has played a crucial role in the EU's policy framework to combat climate change and reduce GHG emissions cost-effectively. The system covers some 10,000 stationary installations, in the energy and industry sectors, and airlines operating in the EU. This represents around 38 percent of the EU's total emissions. In 2021, the EU ETS entered its fourth trading phase (2021-2030). The carbon credit allocation mechanisms have evolved over the four trading phases including auctioning and free-allocation based on benchmarks. The implementation of the Market Stability Reserve (MSR) and Linear Reduction Factor (LRF) policy has caused a drop in the supply of carbon credits, thereby increasing the prices. Therefore, after 2017, the Carbon prices have shown steep increases and significant fluctuations.

As with many other economic and financial indicators, things get complicated. For one, carbon futures have been very volatile since their introduction. One might assume that as the environment gets worse, we would expect futures to grow, putting more pressure on energy companies. Yet situations happen, and simply doing so could lead to other problems. In fact, many times it does not fluctuate as much as we would like it to, but rather fluctuates in response to other indices and events. A recent example of this is the Green Swan event, or "Climate Black Swan". Published by the Bank for International Settlements (BIS) in the report *The green swan Central banking and financial stability in the age of climate change*, a green swan event is defined as a "potentially extremely financially disruptive event that could be behind the next systemic financial crisis" [5]. Specifically, it is an interactive, non-linear, fundamentally unpredictable, potentially irreversible, and complicated dynamic systemic risk [5]. An example of such an event is COVID-19. In general, a green swan event could negatively disrupt current carbon emissions programs. Its impact may be reflected through financial indices such as carbon emissions futures, motivating us to understand it from this perspective.

However, there is always a silver lining to the volatility of financial indices. Even with the disruption of severe weather risk, the introduction of clean solutions to help improve overall emissions can have an impact on carbon futures. One of the most recent clean solutions is Tesla's Powerwall which was introduced in 2015 and further installed in April 2020. The company's stock prices also rose sharply since then. This therefore raises an intriguing topic of determining if there exists a relationship between Tesla stock prices and carbon emissions futures.

The introduction of carbon futures also raises other issues. For example, the credibility of the Carbon Emissions Trading Scheme (CETS) has been questioned as part of the discussion of different carbon policy pricing systems [9]. There have been complaints about the carbon tax that it does not take into account private information and makes the financial mechanism for coping with climate change untrustworthy. For the EU, it does have a very mature market-based system. However, EU energy companies have to worry about their taxing that is not with their foreign competitors [9]. This puts pressure on EU companies because it allows non-EU companies to emit more and it also disrupts the European Green Deal to achieve climate-neutral by 2050. As a result, policymakers have come up with the idea of a Carbon Border Adjustment Mechanism (CBAM) to improve the situation by taxing non-EU energy companies[9]. Once rolled out, this is expected to further disrupt carbon markets.

To sum up, the introduction to carbon markets and carbon emissions futures shows that the topic is not just a climate issue nor a typical financial market, but is much more complicated and there are more factors that we have to take into account. As new policies and variables get introduced in the Phase 4 trading, the classical approaches to studying and predicting carbon prices applicable during Phase 1, 2, and 3, may not be apt presently. Therefore, this paper aims to study the dynamics of the chosen EU carbon emissions futures and to understand how it is affected by real-world events. We will also test two assumptions. We hypothesize that there is a relationship between carbon emissions futures and Tesla stock prices because the introduction of Tesla's energy solutions systematically improves the ways to emit carbon. In addition to this, we also argue that green swan events, particularly COVID-19 around 2020, will cause carbon emissions futures to change systematically. We will examine each hypothesis through our models.

2 Literature Review

Many methods for the analysis of carbon prices and building forecasts for the same have been explored in the past literature. The common approaches attempt to build forecasts for carbon spot

prices as well as future prices using a hybrid approach of utilizing econometric methods alongside machine learning algorithms. Multi-resolution Analysis was also employed by scholars to better understand the carbon price dynamics over short and long periods and appropriate econometric and Machine learning algorithms were then employed. Marc Paolella Et Al analyzed Phase 1 data on EUA spot prices using mixed-normal GARCH models [8]. Their study confirmed the excellent predictive performance of GARCH-type models for data from phase 1 and 2 trading. Zhu and Wei [10] combined the SVM with an ARIMA model and used an optimization algorithm to predict the price of EUA futures during Phase II. Yumeng Huang Et Al. [7] proposed that the non-linear features that have been found for carbon price imply that the traditional forecasting methods, such as ARIMA, GARCH, or other linear models, may not be adequate to model the data accurately. M.E.H. Arouri Et Al. [4] in their paper studied the non-linearities in Carbon spot- futures prices relationships during Phase 2 of EU-ETS.

In this study, we will model Phase 3 and Phase 4 data for carbon futures' prices using econometric methods and understand their advantages and shortcomings. Furthermore, we will comprehensively analyze the establishment of a relationship between Tesla stock price and carbon emission futures, as well as the impact of the Green Swan event, both of which have not been largely involved in previous studies. We will employ relevant models to discuss observations.

3 Data Collection and Analysis

3.1 Analysis of Carbon Emission Price Data

We collected our data from investing.com and Yahoo Finance [2, 3]. For long-term analysis and a comprehensive view, we examined the daily price of EU carbon emissions futures (CFI2Z3) from 2013/01/01 to 2023/12/01. This decade-long dataset would allow us to observe comprehensive patterns in the data. At the same time, we have narrowed our analysis to a selection of prices over the period 2020/01/01 to 2023/12/01 to conduct a short-term analysis and present the most up-to-date information on the market.

To deepen our understanding, we also refer to four influential financial indices for the same period from 2020/01/01 to 2023/12/01: Tesla stock prices, Brent oil futures, the Dow Jones U.S. Oil & Gas Index (DJUSEN), and the S&P Dow Jones Indices (S&P500). They provide the contextual support that allows us to see the broader interactions between carbon markets and the larger financial landscape.

Below is a time-series plot of the carbon emissions futures. As we can see, it has an upward trend and therefore is not covariance stationary, suggesting that a first-order difference may be required. The Autocorrelation Function (ACF) plot shows that all lags are significantly non-zero and hence the time series is non-random. On the other hand, the Partial Autocorrelation Function (PACF) plot shows that the value of the first lag is significantly non-zero, with a few additional lags also showing statistical significance. This suggests a possible fit for an AR(1) model.

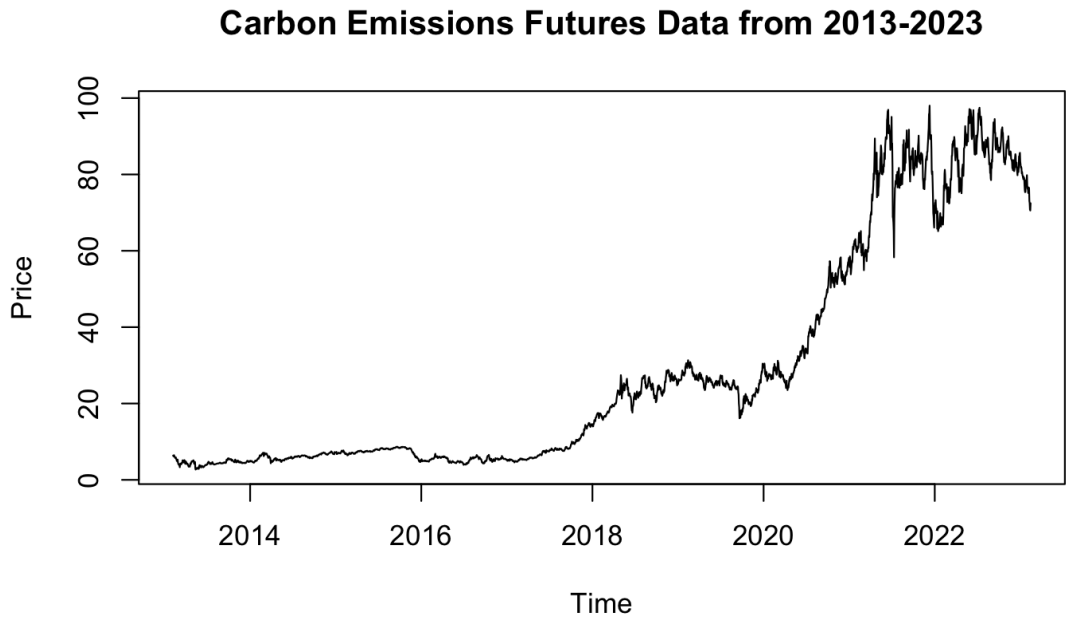

Figure 1. Carbon Emissions Futures Data from 2013-2023

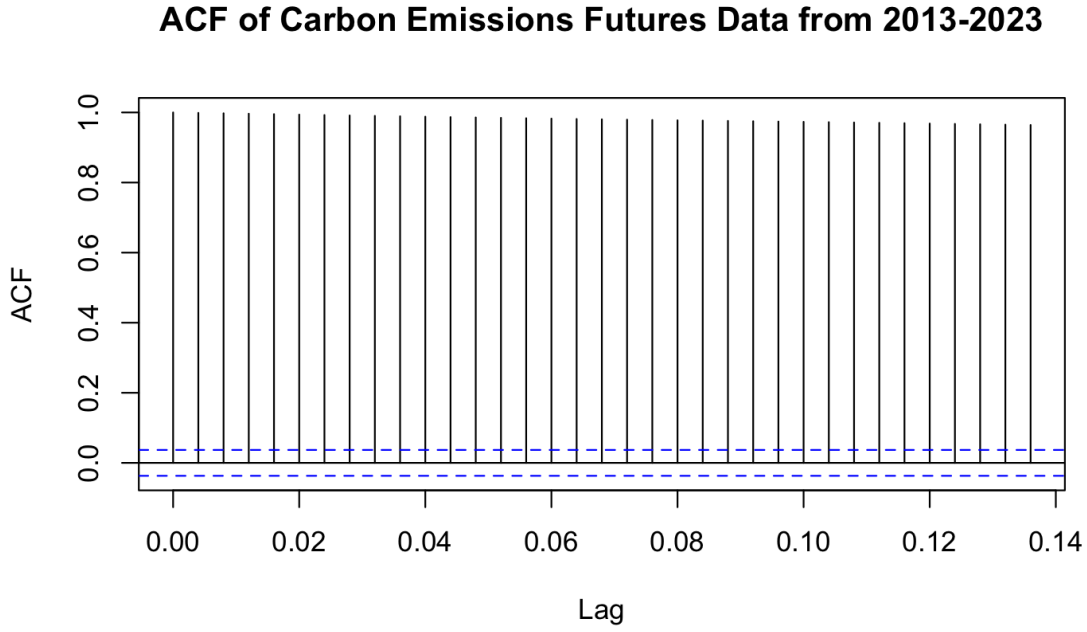

Figure 2. ACF of Carbon Emissions Futures Data from 2013-2023

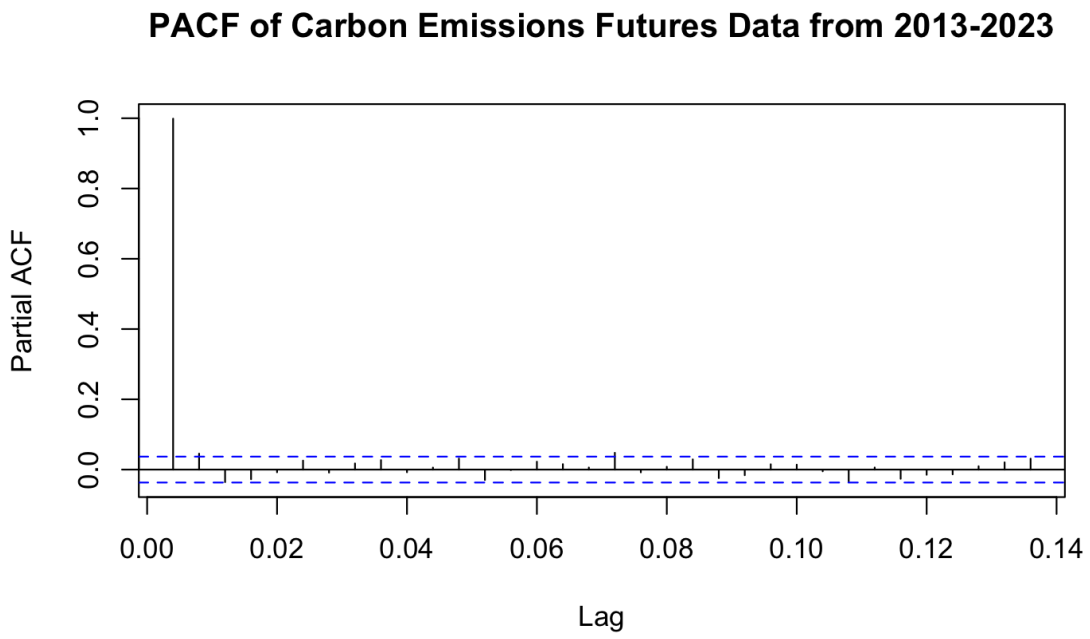

Figure 3. PACF of Carbon Emissions Futures Data from 2013-2023

We then conduct preliminary data analysis by fitting additive and multiplicative decompositions to analyze trend, seasonality, and residuals within data. Mathematically, an additive decomposition refers to $Y_t = S_t + T_t + R_t$ and a multiplicative decomposition refers to $Y_t = S_t \times T_t \times R_t$, where Y_t is the observed value at time t, S_t is the seasonal component, T_t is the trend component, and R_t is the residual. At first glance at the residuals, one would suggest an additive decomposition would be a better fit for the data because the residuals are more random and smaller, whereas the residuals from the multiplicative decomposition seem to have some patterns. The better fit of the additive decomposition also suggests that the data may not have strong seasonal patterns. Indeed, as we can see from the seasonal component plot of the additive decomposition, the oscillations throughout the year are small, although they are lower at the beginning and end of the year.

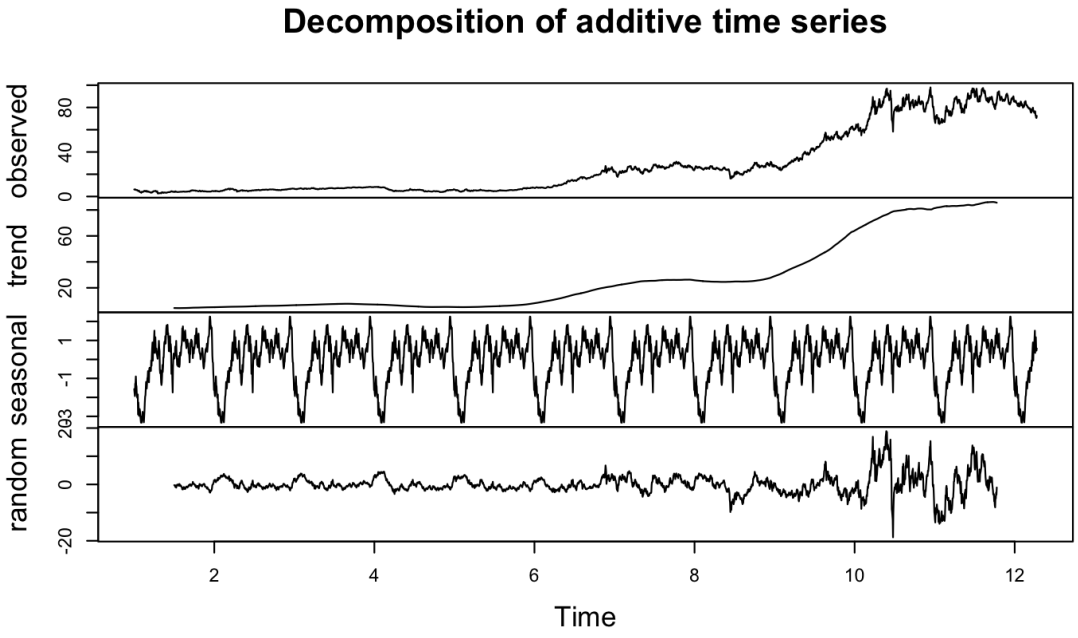

Figure 4. Decomposition of additive time series

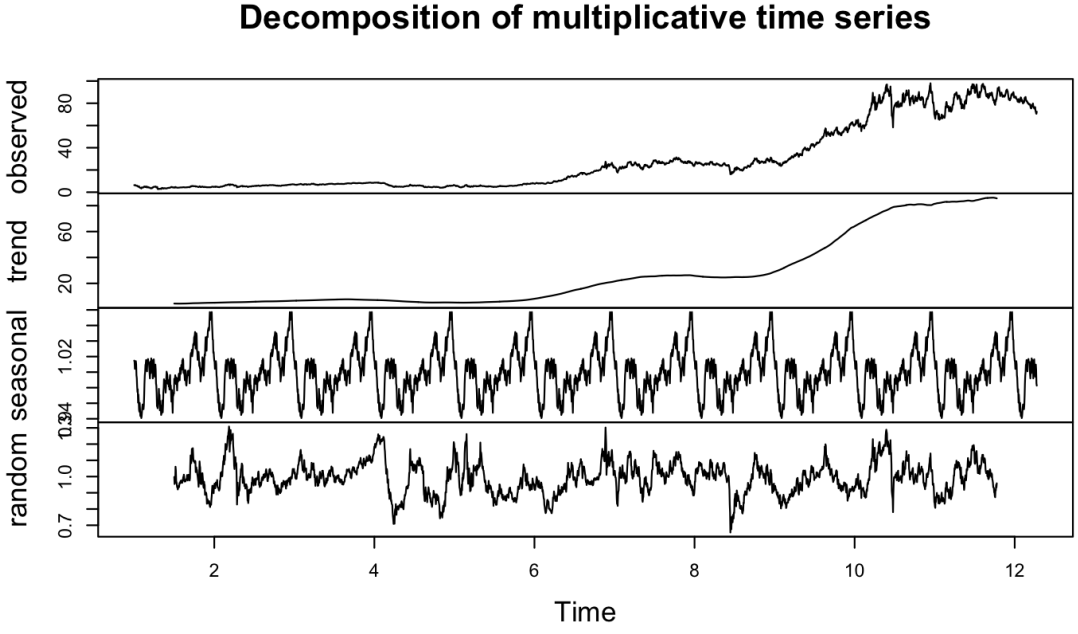

Figure 5. Decomposition of multiplicative time series

Therefore, our preview of the carbon emissions futures data suggests the use of stochastic and deep-learning models because they are good at capturing non-random features of data and data feature selection.

3.2 Analysis of Log returns of Price of Carbon Emissions Futures

Further, we analyze the log-returns of Carbon futures price data. For this, we consider the data from Phase-3 trading onward- between 2017 and 2023. We plot the Time series realizations of log returns of the Carbon emissions futures prices from 2017-2023 in **Figure 6**

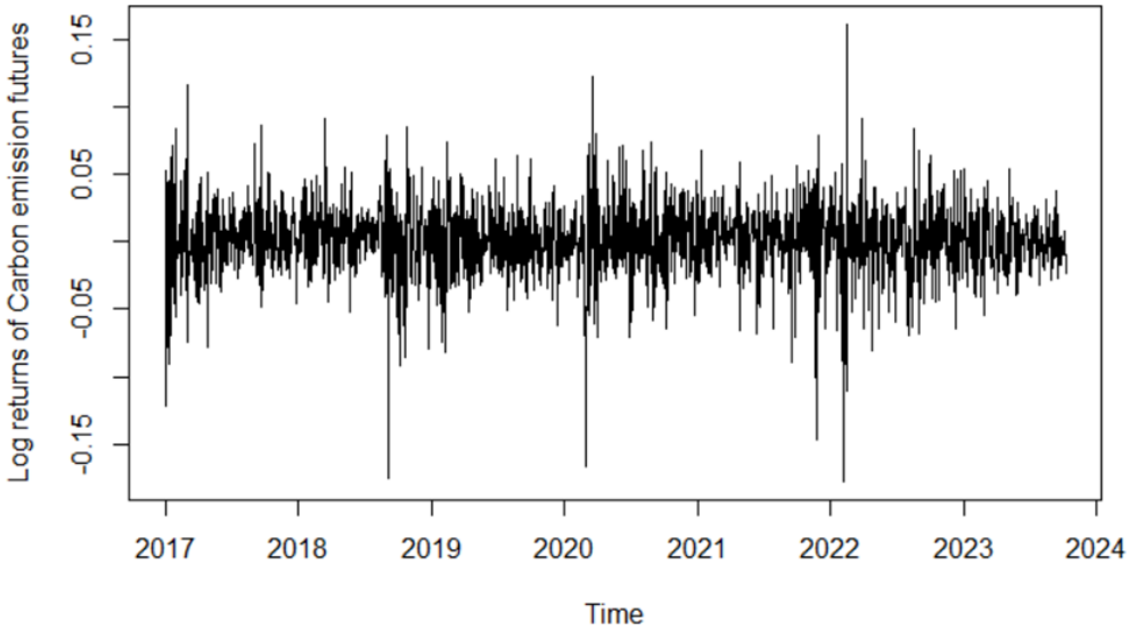

Figure 6 . Time Series Plot for log returns of carbon emission futures during 2017-2023

Generally, the mean of the time series for log returns of carbon emission futures is close to zero; the volatility of the series is fairly uniform during 2017-2023. However, the volatility of the log returns series was highly non-uniform and more pronounced around mid-2018, 2020 and 2022.

3.2.1 Exploratory Data Analysis and Descriptive Statistics

The data is based on daily prices of carbon emission futures for the period during 2017-2023. The time series analysis for the log returns of carbon emission futures is plotted using the logarithm of the returns of the rates, as shown above.

We define p_t as the prices at time t, and p_{t-1} are the prices at time $t-1$. Then the logarithm of the returns is given as:
$R_t = \log\left(\frac{p_t}{p_{t-1}}\right)$ where,

$$R_t = \text{Log Return}, \quad p_t = \text{Current rate}, \quad p_{t-1} = \text{Previous day rate}$$

The log returns are usually assumed to follow a normal distribution which makes all computations easier. A histogram or the density plot of log returns below illustrating a bell shape, an indication of the normality assumption. In addition, log returns time series are usually stationary which can be easier to predict than the non-stationary time series with wild volatility.

The summary statistics and density plot of the log returns of carbon emission futures are shown below.

Table 1: Summary Statistics of log returns of carbon emission futures

Min	1st Q	Median	Mean	3rd Q	Max
-0.1773	-0.01358	0.001656	0.001402	0.018263	0.161378

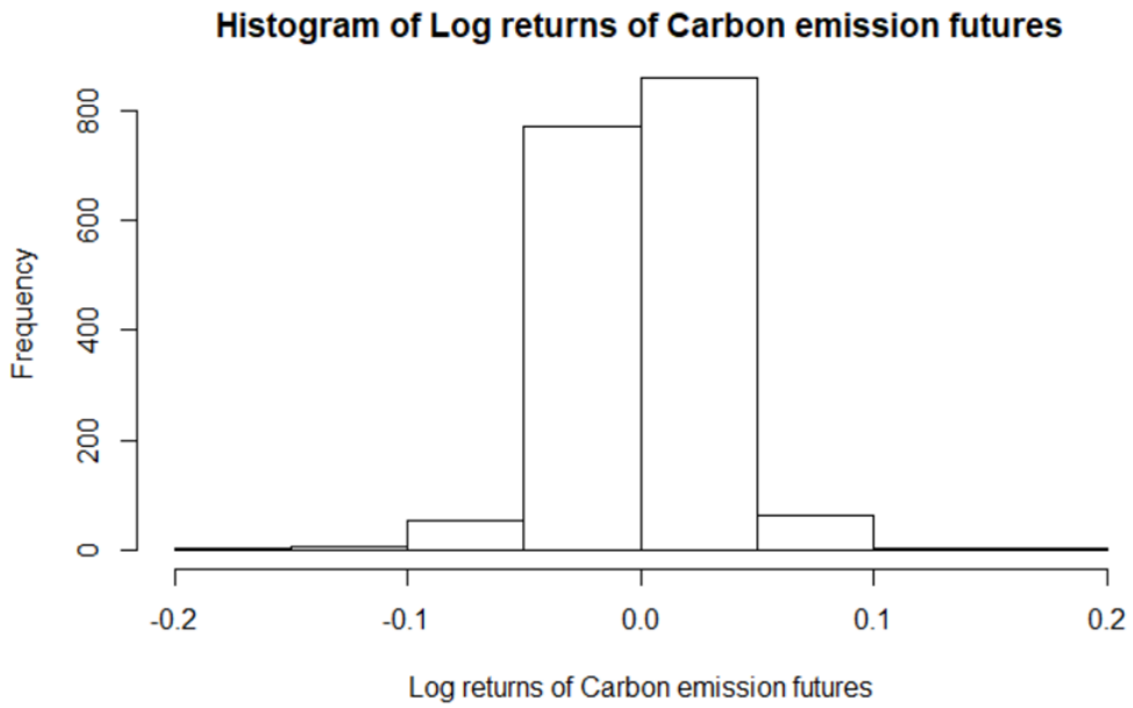

Figure 7. Time Series Plot for log returns of carbon emission futures during 2017-2023

The slightly negative skewness value, which shown from the fact that the mean is slightly less than the median, confirms the presence of asymmetries within the log returns of carbon emission futures distribution.

The time series plot for daily prices of carbon emission futures does not exhibit periodicity but we do see an upward trend effect. After transforming data to log returns, the trend effect is eliminated. Therefore, we do not need to apply any differencing technique to make the series stationary and the integration order should be zero.

4 Analysis Methods and Modelling

4.1 Long-Term Approaches for Carbon price data

Building directly on the above simple analysis in Section 3.1, we would suggest an ARIMA (AutoRegressive Integrated Moving Average) model. The ARIMA model is a common approach when it comes to daily financial prices, as it captures MA (moving average) and AR (autoregression) with differencing (for making data covariance stationary) as well as taking into account seasonal components of MA, AR, and differences. Here we provide a formal mathematical representation of MA and AR:

Definition 4.1 *MA of order* $q := MA(q)$*:* $Y_t = \mu + \sum_{i=1}^{q} \theta_i \epsilon_{t-i}$*, where* $\epsilon_t \sim (0, \sigma^2)$.

Definition 4.2 *AR of order* $p := AR(p)$*:* $Y_t = c + \sum_{i=1}^{q} \phi_i Y_{t-i} + \epsilon_t$*, where* $\epsilon_t \sim (0, \sigma^2)$.

Definition 4.3 *Seasonal AR of order* $p := S - AR(p)$.

Definition 4.4 *Seasonal MA of order* $q := S - MA(q)$.

In addition to the ARIMA model, we propose to use an NNETAR (neural network autoregressive) model because we would like to explore autoregression more and because the model might be useful for data feature selection. NNETAR employs a non-linear autoregressive structure and predicts values based on their past values and inputs by adding activation functions to hidden layers and adjusting the weights of the neural network to minimize differences. The following equation describes the NNETAR process for computation within a neural network layer:

$$Y_t = f(\sum_{i=1}^{n} w_{hi} \cdot h_i + b_h)$$

where Y_t is the predicted value at time t, f is the activation function to the sum of weighted inputs, n is the number of hidden neurons in the neural network, h_i is the output of hidden layer neurons, w_{hi} are the weights connecting the i-th neuron from the previous layer to the t-th neuron in the current layer, and b_h is the bias term for the current hidden layer.

Moreover, considering the outliers within the data, a Prophet model is chosen. Prophet is a time series forecasting model developed by Facebook (Meta). It is a linear function that combines trend, seasonality, and holiday effects. A mathematical illustration is here:

$$Y_t = g(t) + s(t) + h(t) + \epsilon_t$$

where $g(t)$ is the trend, $s(t)$ is the seasonality, $h(t)$ is the holiday effect, and ϵ_t is the error term.

To be specific, the trend is modeled through a piecewise linear model with changepoints. We define $g(t) := \sum_{i=1}^{n}(k_i \cdot I(t \geq \tau_i))$, where k_i is the slope of the trend between changepoints τ_i and $I(t \geq \tau_i)$ is an indicator function. In addition, the model handles seasonality through Fourier series expansion. We therefore have our seasonality component as $s(t) := s_{yearly}(t) + s_{weekly}(t)$, where $s_{yearly}(t) = \sum_{i=1}^{n}(a_i \cdot cos(\frac{2\pi it}{p}) + b_i \cdot sin(\frac{2\pi it}{p}))$ for p as the period of the seasonality component and $s_{weekly}(t) = \sum_{i=1}^{n}(c_i \cdot cos(\frac{2\pi it}{7}) + d_i \cdot sin(\frac{2\pi it}{7}))$.

However, since there is not much seasonality, we do not expect Prophet to be the best-fitted model among all. Nevertheless, the checkpoint feature of Prophet might give insights into where the data is more predictable, as well as some financial inspirations. As such, it is a good complement to the previous two models.

In brief, from the descriptions of these three models, we can see that they all have their own strengths and are a bit different in logic. As a result, these three models are expected to provide good prediction and a relatively comprehensive understanding of the carbon futures.

4.2 Short-Term Approaches for Carbon Price data

For short-term analysis, we wish to take a step further from simply regressing carbon futures on itself, but also incorporating other financial indexes described above to see how they interact with each other. Therefore, we will use linear regression as a benchmark because it is simple and powerful and lends to straightforward interpretation. We first apply a VAR (Vector Autoregression) analysis on five datasets. A mathematical representation of a VAR model is incorporated below:

$$Y_t = \beta_0 + \sum_{i=1}^{n}\sum_{j=0}^{p} \beta_i X_{t-j,i} + \epsilon_t$$

where p is the number of lags and n is the number of dependent variables.

If relationships were shown in the VAR model, we could set up a more targeted linear regression of a similar form (but with more flexibility in terms of the degree of lags and the number of dependent variables). However, given the highly intertwined and interacting nature of the financial indices, we expect multicollinearity to occur. Therefore, linear regression alone is not sufficient and we may correct this by using PCA (Principal Component Analysis), a widely used machine learning technique that extracts important features and reduces noise by transforming high-dimensional datasets into low-dimensional ones. It uses linear algebra, which involves normalizing the raw data to obtain a covariance matrix for the data and then applying an eigenvalue decomposition. Based on this, PCA selects principal components by choosing the top k eigenvectors corresponding to the largest k eigenvalues. Then a projection is applied, i.e. $Y = ZW_k$, Z is the normalized matrix and W_k is the matrix of selected eigenvectors, so Y is the reduced dimensionality dataset. While this method is efficient, we shall keep in mind that Y is much harder to interpret than variables in linear regression, but we can test how much we can reduce the error for our dataset.

An IV (Instrumental Variable) regression can also be employed to address endogeneity (correlation) problems. IV distinguishes between exogenous and endogenous variables, which are variables that are correlated with the error term that disturb the bias and consistency of linear regression. An IV model can be expressed as $Y = \alpha_0 + \alpha_1(\hat{X}) + \epsilon$ for $X = \pi_0 + \pi_1 Z + \zeta$ where $\hat{X}$ is the predicted value from the latter regression. Here Z is the instrumental variable associated with X and Y is the endogenous variable.

To sum up, as we wish to apply various financial indices, we propose a few other models, namely linear regression, VAR, PCA, and IV regression. We expect that at least a combination of linear regression and PCA analysis will explain the problem well.

4.3 Modelling Log-returns data for Price of Carbon Emission futures

4.3.1 ARMA

The ARMA model comprises two distinct processes: Autoregressive (AR) and Moving Average (MA). The AR component models the current observation level based on its lagged observations, representing a dependence on past values. Meanwhile, the MA component captures the fact that observations at time t are influenced not only by the shock at the time t but also by shocks occurring prior to time t. This framework allows us to model the future of the time series based on the past, the present of the variable and previous shocks that influenced the variable. ARIMA is one of the most traditional methods to estimate and project time series. In contrast to the regression models, the ARIMA model allows time series to be explained by its past or lagged values and stochastic error terms. The models developed by this approach are usually called ARIMA models because they use a combination of autoregressive (AR), integration (I) - referring to the reverse process of differencing to produce the forecast and moving average (MA) operations (Box, G.E.P. and Jenkins, G.M. 1970).

The general model for Yt is written as:

$Y_t = \phi_1 Y_{t-1} + \phi_2 Y_{t-2} + \ldots + \phi_p Y_{t-p} + \epsilon_t + \theta_1 \epsilon_{t-1} + \theta_2 \epsilon_{t-2} + \ldots + \theta_q \epsilon_{t-q}$

where Y_t is the differenced time series value, ϕ and θ are unknown parameters, and ε are independent identically distributed error terms with zero mean. Y_t is written in terms of its past values and the current and past values of error terms. The ARIMA (p,d,q) model contains three main parts:

A) Auto Regression (AR): the dependent variable or a given time series data are regressed on their own lagged values, which is expressed by the "p" value in the model.

B) Differencing (I-for Integrated): involves differencing the time series data to remove the deterministic trend and convert a non-stationary time series to a stationary time series. This is indicated by the "d" value in the model. If d = 1, it looks at the difference between two time series entries, if d = 2 it looks at the differences of the differences obtained at d =1, and so forth.
C) Moving Average (MA): the moving average nature of the model is represented by the "q" value which is the number of lagged values of the error term.

We split the data into Training set (2017-2022) and Testing set (2022-2023). All further analysis in this section is done on Training Set. We compare the model against the testing data to conclude the goodness of fit.

First, we will test stationarity and identify ARIMA(p,d,q) appropriate model for forecasting. To build an ARIMA model, the following steps will be implemented:
(I) Test for Stationarity
(II) Identify parameters of ARIMA (p,d,q)
We can identify the appropriate order of Autoregressive (AR) and Moving average (MA) processes by using the Autocorrelation function (ACF) and Partial Autocorrelation function (PACF).
1. Identifying the p order of AR model
For AR models, the ACF will decay or dampen exponentially and the PACF will be used to identify the order (p) of the AR model. If we have one significant spike at lag 1 on the PACF, then we have an AR model of the order 1, i.e. AR(1). If we have significant spikes at lag 1, 2, and 3 on the PACF, then we have an AR model of the order 3, i.e. AR(3).
2. Identifying the q order of MA model
For MA models, the PACF will decay or dampen exponentially and the ACF plot will be used to identify the order of the MA process. If we have one significant spike at lag 1 on the ACF, then we have an MA model of the order 1, i.e. MA(1). If we have significant spikes at lag 1, 2, and 3 on the ACF, then we have an MA model of the order 3, i.e. MA(3).
3. Model Estimation and Forecasting, Diagnostic Checking
Once we have determined the parameters (p,d,q), we estimate the accuracy of the ARIMA model on a training data set and then use the fitted model to forecast the values of the test data set using a forecasting function. In the end, we cross check whether our forecasted values are in line with the actual values.
4. Forecasting evaluation metrics
To check the model fit and perform model diagnostics, the dataset on log returns of carbon emission futures was split into training and testing data where the training data was from January 2017 to December 2022 and the testing data was from January 2023 to November 2023. Comparison among family of different parametric combination of ARIMA (p, d, q) was done on the basis of minimum value of selection criteria which is AIC.

The Autocorrelation Function (ACF) and Partial Autocorrelation Function (PACF) are used to determine the orders of the AR and MA processes respectively.

4.3.2 GARCH (Generalized Autoregressive Conditional Heteroskedasticity):

GARCH is a statistical model that extends the ARCH (Autoregressive Conditional Heteroskedasticity) model by introducing a dynamic component that models the conditional variance of a time series as a linear combination of past squared observations and past conditional variances. GARCH models are particularly useful for modeling the changing volatility in financial markets.

GARCH (Generalized Autoregressive Conditional Heteroskedasticity) process is a process where

the conditional mean is constant but the conditional variance is non-constant and hence an uncorrelated but dependent process. The Volatility σ^2 is modelled as an ARMA(p,q) process. The ARMA(p,q) formulation in a GARCH process is :

$$\sigma_t^2 = \omega + \sum_{i=1}^{p} \alpha_i \varepsilon_{t-i}^2 + \sum_{j=1}^{q} \beta_j \sigma_{t-j}^2$$

where

$$\sigma_t^2 > 0 \quad \text{if and only if} \quad \omega > 0 \quad \text{and} \quad \alpha_i \geq 0 \quad (i = 1, \ldots, p) \quad \text{and} \quad \beta_j \geq 0 \quad (j = 1, \ldots, q)$$

4.3.3 EGARCH (Exponential Generalized Autoregressive Conditional Heteroskedasticity):

EGARCH is an extension of the GARCH model that allows for asymmetric responses to positive and negative shocks. Unlike GARCH, EGARCH models the logarithm of the conditional variance, introducing an asymmetric response parameter that captures the leverage effect. The leverage effect implies that negative shocks tend to have a stronger impact on volatility than positive shocks of the same magnitude. The exponential GARCH (eGARCH) variance model is capable of capturing asymmetries within the volatility shocks.

The volatility is modelled as follows:

$$\ln(\sigma_t^2) = \omega + \sum_{j=1}^{q} \left(\alpha_j \varepsilon_{t-j}^2 + \gamma(\varepsilon_{t-j} - E|\varepsilon_{t-j}|) \right) + \sum_{i=1}^{p} \beta_i \ln(\sigma_{t-i}^2)$$

where Y_t is the log returns of carbon emission futures ϵ_t is the shock and ϵ_t $\text{WN}(0,\sigma_t^2)$ σ_t^2 is the volatility ω , α , β are coefficients that will be estimated.

The volatility component is used to scale the noise term in the ARMA process as follows:

$$u_t = \sigma_t \epsilon_t$$

4.3.4 Maximum Likelihood Estimation

We use the Maximum Likelihood Estimator to estimate the parameters of the GARCH/EGARCH models.

Let $X_1, \ldots, X_T$ be an i.i.d. sample with probability density function (pdf) $f(x_t; \theta)$, where θ is a $(k \times 1)$ vector of parameters that characterize $f(x_t; \theta)$. For example, if $X_t \sim \mathcal{N}(\mu, \sigma^2)$ then $f(x_t; \theta) = (2\pi\sigma^2)^{-1/2} \exp\left(-\frac{1}{2\sigma^2}(x_t - \mu)^2\right)$ and $\theta = (\mu, \sigma^2)'$. The joint density of the sample is, by independence, equal to the product of the marginal densities

$$f(x_1, \ldots, x_T; \theta) = f(x_1; \theta) \cdots f(x_T; \theta) = \prod_{t=1}^{T} f(x_t; \theta).$$

The joint density is a T-dimensional function of the data $x_1, \ldots, x_T$ given the parameter vector θ. The joint density satisfies

$$f(x_1, \ldots, x_T; \theta) \geq 0, \quad \int \cdots \int f(x_1, \ldots, x_T; \theta)\, dx_1 \cdots dx_T = 1.$$

Then, the Likelihood function, which is a function of θ is defined as the joint probability density

$$L(\theta|x_1, \ldots, x_T) = f(x_1, \ldots, x_T; \theta) = \prod_{t=1}^{T} f(x_t; \theta)$$

The MLE for θ, denoted $\hat{\theta}_{\text{MLE}}$, is the value of θ that maximizes $L(\theta|x)$. That is, $\hat{\theta}_{\text{MLE}}$ solves the optimization problem

$$\max_{\theta} L(\theta|x).$$

Since $\ln(\cdot)$ is a monotonically increasing function, the value of θ that maximizes $\ln L(\theta|x)$ will also maximize $L(\theta|x)$. Therefore, we may also define $\hat{\theta}_{\text{MLE}}$ as the value of θ that solves

$$\max_{\theta} \ln L(\theta|x).$$

With random sampling, the log-likelihood is additive in the log of the marginal densities:

$$\ln L(\theta|x) = \ln \left(\prod_{t=1}^{T} f(x_t; \theta) \right) = \sum_{t=1}^{T} \ln f(x_t; \theta).$$

For a covariance stationary time series, the conditional log-likelihood is additive in the log of the conditional densities:

$$\ln L(\theta|x) = \ln \left(\prod_{t=1}^{T} f(x_t|I_{t-1}; \theta) \right) = \sum_{t=1}^{T} \ln f(x_t|I_{t-1}; \theta).$$

We find the MLE by differentiating $\ln L(\theta|x)$ and solving the first-order conditions

$$\frac{\partial \ln L(\hat{\theta}_{\text{MLE}}|x)}{\partial \theta} = 0.$$

In some cases, it is possible to find analytic solutions to the set of equations $S(\hat{\theta}_{\text{MLE}}|x) = 0$. However, for ARCH and GARCH models, the set of equations $S(\hat{\theta}_{\text{MLE}}|x) = 0$ are complicated nonlinear functions of the elements of θ and no analytic solutions exist. As a result, numerical optimization methods are required to determine $\hat{\theta}_{\text{MLE}}$.

5 Results

5.1 Long-Term Analysis

5.1.1 ARIMA

As expected, ARIMA gives us an "all-encompassing" model that incorporates the fluctuations we described above. We see that the best-fitting model is ARIMA$(1,1,0)(0,0,1)[250]$ with drift. The model consists of a first-order differentiation, AR(1), S-MA(1), and a drift coefficient. To illustrate, the AR(1) coefficient $ar1 = -0.0554$ indicates that the series is negatively correlated with its previous value so that when the previous value decreases, the current value tends to increase. The S-MA(1) coefficient $sma1 = 0.0380$ suggests a positive correlation of seasonal moving averages, so we expect the seasonal pattern to increase for every 250 observations. The drift coefficient $drift = 0.0231$ shows a positive linear trend in the data. All coefficients are small in magnitude,

indicating a weak impact for each model. In addition, since we have a low RMSE= 1.122177 and ACF1= 0.003318835, this suggests that their combination fits the data well.

```
Series: Carbon_ts
ARIMA(1,1,0)(0,0,1)[250] with drift

Coefficients:
          ar1    sma1   drift
      -0.0554  0.0380  0.0231
s.e.   0.0188  0.0206  0.0207

sigma^2 = 1.261:  log likelihood = -4325.62
AIC=8659.24   AICc=8659.25   BIC=8683.01

Training set error measures:
                      ME     RMSE       MAE        MPE     MAPE       MASE
Training set 4.718616e-05 1.122177 0.5778578 -0.196247 2.175924 0.06295372
                    ACF1
Training set 0.003318835
```

Figure 8. ARIMA

5.1.2 NNETAR

NNETAR has a structure of a 4-2-1 network with 13 weights. We have a neural network autoregressive model with 4 lagged inputs and 2 hidden units in a hidden layer. From the comparison of performance metrics, especially that RMSE= 1.106561, NNETAR slightly outperforms ARIMA.

```
Series: Carbon_xts
Model:  NNAR(4,2)
Call:   nnetar(y = Carbon_xts)

Average of 20 networks, each of which is
a 4-2-1 network with 13 weights
options were - linear output units

sigma^2 estimated as 1.222
                       ME     RMSE       MAE         MPE     MAPE      MASE
Training set -0.002128385 1.105607 0.5728139 -0.1905576 2.171316 0.9908827
                     ACF1
Training set -0.0007957652
```

Figure 9. NNETAR

5.1.3 Prophet

For the Prophet model, we use a rolling window for forecasting. We see that the model fits the data well up to 2022, especially the growth from 2020 to 2022, but it fails to capture the data after 2022. Through the decomposition, we find that it provides more information on yearly changes. For example, it shows prices starting to fall in September and rising in February. The performance

metrics get worse as we forecast over a longer period, where an increase in the forecast horizon leads to an increase in the forecast error, and long-term forecasts are usually more volatile. This result shows an advantage of HFT (High-Frequency Trading) as short-term forecasts are more stable and less risky. This is true not only in traditional financial markets but also in the carbon market. In addition, it provides us with a reason that we need to look more closely at the data for 2020 to 2023 to perform short-term analysis.

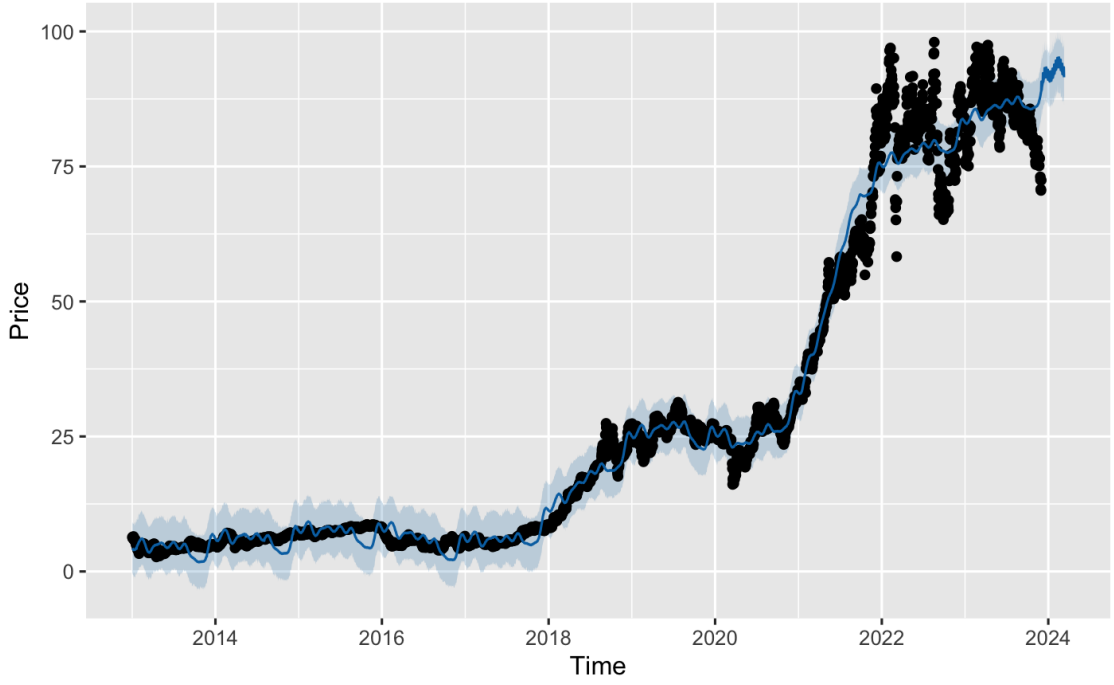

Figure 10. Prophet Forecasting

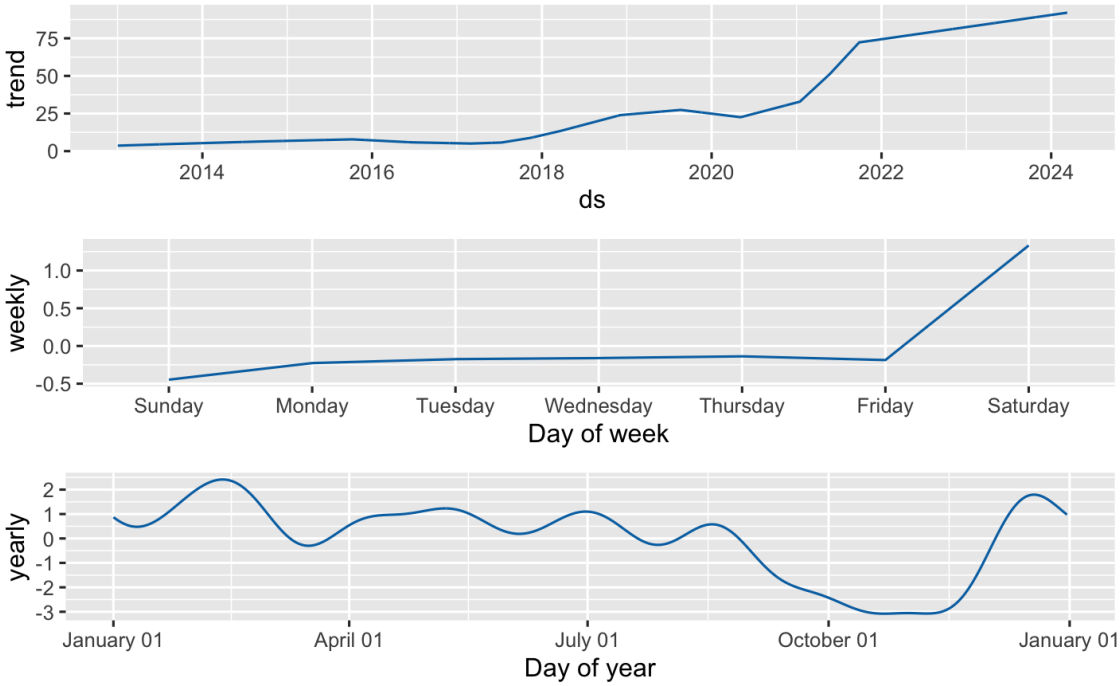

Figure 11. Components of Prophet

	horizon	mse	rmse	mae	mape	mdape	smape	coverage
1	10 days	44.58054	6.676866	4.211846	0.1305795	0.1104775	0.1319389	0.3306329
2	11 days	44.84171	6.696395	4.260533	0.1339213	0.1141489	0.1355290	0.3293413
3	12 days	45.06999	6.713418	4.272120	0.1373568	0.1206375	0.1391424	0.3265868
4	13 days	47.43316	6.887174	4.377205	0.1425713	0.1240495	0.1442525	0.3113772
5	14 days	50.13136	7.080350	4.499246	0.1464885	0.1286582	0.1481812	0.2926799
6	15 days	50.87282	7.132519	4.522070	0.1483203	0.1286582	0.1498330	0.2860162

Figure 12. Prophet Performance Metrics

In brief, ARIMA and NNETAR both provide good estimates of the data with NNETAR a slightly more accurate model, and with Prophet, we see a systematic change for data after 2022 and get more information about how training time affects prediction accuracy, which motivates us to perform short-term analyses.

5.2 Short-Term Analysis

5.2.1 VAR

We estimated the VAR model as

$$\begin{aligned} Carbon_t = {} & 13.582107 + 0.964338 \times Carbon_{t-1} - 0.168411 \times Brent_{t-1} + 0.031462 \times TSLA_{t-1} \\ & + 0.040708 \times DJUSEN_{t-1} - 0.005486 \times S\&P500_{t-1} - 0.036617 \times Carbon_{t-2} \\ & + 0.011506 \times Brent_{t-1} - 0.011982 \times TSLA_{t-2} - 0.016854 \times DJUSEN_{t-2} \\ & + 0.001822 \times S\&P500_{t-2} \end{aligned}$$

	Estimate	Std. Error	t value	Pr(>|t|)	
Carbon.l1	0.964338	0.070653	13.649	<2e-16	***
BZ.F.Close.l1	-0.168411	0.105831	-1.591	0.1131	
TSLA.Close.l1	0.031462	0.019867	1.584	0.1149	
DJUSEN.l1	0.040708	0.017741	2.295	0.0228	*
GSPC.Close.l1	-0.005486	0.004481	-1.224	0.2223	
Carbon.l2	-0.036617	0.070976	-0.516	0.6065	
BZ.F.Close.l2	0.011506	0.103326	0.111	0.9114	
TSLA.Close.l2	-0.011982	0.020064	-0.597	0.5511	
DJUSEN.l2	-0.016854	0.017730	-0.951	0.3430	
GSPC.Close.l2	0.001822	0.004518	0.403	0.6871	
const	13.582107	6.646517	2.043	0.0423	*

Signif. codes: 0 '***' 0.001 '**' 0.01 '*' 0.05 '.' 0.1 ' ' 1

Residual standard error: 1.84 on 200 degrees of freedom
Multiple R-Squared: 0.8948, Adjusted R-squared: 0.8896
F-statistic: 170.2 on 10 and 200 DF, p-value: < 2.2e-16

Figure 13. VAR Model Results

The VAR model provides us with information on linear regressions of carbon emissions futures to various lagged values. In the VAR model, we still see a strong relationship between carbon emissions futures and its own lagged values (not in terms of the magnitude of the estimate, but in terms of statistical significance since its p-value is $< 2e-16$), but not with the other lagged values. Lag 1 of DJUSEN has a certain degree of statistical significance since the p-value of its estimate is < 0.05. However, a high $R^2 = 0.8948$ of the VAR model suggests that variables are statistically insignificant due to multicollinearity among them ($VIF > 1$) which needs further analysis.

We then use the Granger causality test, which is a statistical hypothesis test used to determine whether one time series helps to predict another. After testing and tracing, we find that the lagged 6-period relationship between Tesla stock price and carbon emission futures is relatively strong because of its p-value < 0.05. Therefore, we can consider the lagged 6 periods of Tesla stock price for forecasting carbon emission futures.

```
Granger causality test

Model 1: Carbon_ts ~ Lags(Carbon_ts, 1:6) + Lags(tsla_ts, 1:6)
Model 2: Carbon_ts ~ Lags(Carbon_ts, 1:6)
  Res.Df Df     F  Pr(>F)
1    194
2    200 -6 2.187 0.04586 *
---
Signif. codes:  0 ‘***’ 0.001 ‘**’ 0.01 ‘*’ 0.05 ‘.’ 0.1 ‘ ’ 1
```

Figure 14. Granger Causality Test Result

Therefore, the VAR model here sets a good benchmark and the linear relationship it reveals is worth exploring further.

5.2.2 Linear Regression and PCA

Based on the VAR model above, we select a nice linear regression as below:

$$Carbon_t = 9.348537 + 0.946187 \times Carbon_{t-1} + 0.032055 \times TSLA_t - 0.015963 \times TSLA_{t-6} - 0.103238 \times Brent_t + 0.021104 \times DJUSEN_t - 0.003461 \times S\&P500_t$$

```
Time series regression with "ts" data:
Start = 1(7), End = 1(213)

Call:
dynlm(formula = Carbon_ts ~ L(Carbon_ts, 1) + tsla_ts + L(tsla_ts,
    6) + brent_ts + DJUSEN_ts + sp500_ts)

Residuals:
    Min      1Q  Median      3Q     Max
-4.9218 -1.2180  0.0269  1.3230  4.4920

Coefficients:
                 Estimate Std. Error t value Pr(>|t|)
(Intercept)      9.348537   6.490565   1.440 0.151338
L(Carbon_ts, 1)  0.946187   0.026655  35.497  < 2e-16 ***
tsla_ts          0.032055   0.008550   3.749 0.000232 ***
L(tsla_ts, 6)   -0.015963   0.006771  -2.358 0.019361 *
brent_ts        -0.103238   0.067675  -1.526 0.128713
DJUSEN_ts        0.021104   0.010504   2.009 0.045866 *
sp500_ts        -0.003461   0.001451  -2.385 0.018023 *
---
Signif. codes:  0 ‘***’ 0.001 ‘**’ 0.01 ‘*’ 0.05 ‘.’ 0.1 ‘ ’ 1

Residual standard error: 1.826 on 200 degrees of freedom
Multiple R-squared:  0.896,     Adjusted R-squared:  0.8929
F-statistic: 287.3 on 6 and 200 DF,  p-value: < 2.2e-16
```

Figure 15. Linear Regression

```
L(Carbon_ts, 1)        tsla_ts   L(tsla_ts, 6)        brent_ts       DJUSEN_ts
       1.319349        9.077501        5.666682        8.100932        7.400990
       sp500_ts
       6.179630
```

Figure 16. VIF Analysis of Linear Regression

As we can easily see, the linear model has a very high $R^2 = 0.896$ while utilizing only a few variables. Some statistical significance shows for Tesla, lag 6 of Tesla, DJUSEN, and S& P500. An increase in a unit of lag 6 of Tesla tends to lead to a decrease of 0.015963 unit of carbon futures, and an increase in a unit of Teslat tends to lead to an increase of 0.032055 of carbon futures. Multicollinearity clearly exists as we test their VIFs, so we use a PCA transform. Then, we regress carbon emissions futures on the 3 most important PCA components. The new model gives us an $R^2 = 0.9946$, an almost perfect fit, which tells us that we can forecast short-term carbon emissions futures through current datasets. However, we do not know how to characterize PCA components, so this can be an interesting future topic.

```
Importance of components:
                          PC1    PC2    PC3    PC4     PC5      PC6
Standard deviation     1.7267 1.3512 0.9881 0.3842 0.26240 7.17e-16
Proportion of Variance 0.4969 0.3043 0.1627 0.0246 0.01148 0.00e+00
Cumulative Proportion  0.4969 0.8012 0.9639 0.9885 1.00000 1.00e+00
```

Figure 17. PCA

```
Call:
lm(formula = Carbon_ts ~ PC1 + PC2 + PC3, data = pc_data)

Residuals:
     Min       1Q   Median       3Q      Max
-1.00232 -0.30502 -0.00133  0.34184  0.77645

Coefficients:
            Estimate Std. Error t value Pr(>|t|)
(Intercept) 85.80418    0.02806 3058.18   <2e-16 ***
PC1          0.66383    0.01629   40.76   <2e-16 ***
PC2         -1.02548    0.02081  -49.27   <2e-16 ***
PC3          5.25804    0.02846  184.73   <2e-16 ***
---
Signif. codes:  0 ‘***’ 0.001 ‘**’ 0.01 ‘*’ 0.05 ‘.’ 0.1 ‘ ’ 1

Residual standard error: 0.4095 on 209 degrees of freedom
Multiple R-squared:  0.9946,    Adjusted R-squared:  0.9945
F-statistic: 1.274e+04 on 3 and 209 DF,  p-value: < 2.2e-16
```

Figure 18. Linear Regression Results Using PCA Components

5.2.3 IV Regression

Due to the dependence of variables, we are intrigued to use some variables as endogenous. But we do not see much "simpleness" here. An example of a poorly fitted IV regression is shown below. Here, we can see that $R^2 < 0$, which suggests that IV regressions may not be appropriate.

```
Call:
ivreg(formula = Carbon_ts ~ tsla_ts + brent_ts | DJUSEN_ts +
    sp500_ts)

Residuals:
     Min       1Q   Median       3Q      Max
-14.2242  -3.2307   0.5654   3.3823  11.5615

Coefficients:
             Estimate Std. Error t value Pr(>|t|)
(Intercept) 106.30016    6.73593  15.781  < 2e-16 ***
tsla_ts      -0.03010    0.01004  -2.998  0.00305 **
brent_ts     -0.17252    0.08172  -2.111  0.03595 *
---
Signif. codes:  0 ‘***’ 0.001 ‘**’ 0.01 ‘*’ 0.05 ‘.’ 0.1 ‘ ’ 1

Residual standard error: 5.637 on 210 degrees of freedom
Multiple R-Squared: -0.03564,   Adjusted R-squared: -0.0455
Wald test: 7.965 on 2 and 210 DF,  p-value: 0.0004633
```

Figure 19. IV Regression

In short, our short-term analysis reveals relationships between carbon futures and financial metrics. The perfection of PCA suggests that the likelihood of carbon futures prediction is mostly explainable through different financial datasets, even during periods of volatile data. Furthermore, the relationship between Tesla stock prices and especially their lags and carbon emissions futures is recognized. However, models with a simpler interpretation might be needed in the future.

5.3 Model for Log Returns of Carbon Emission Futures

We first apply ARMA modeling technique to a time series data, where the time series of log returns of carbon emission futures is a stationary process. The logarithm of returns of the carbon emission futures are stationary, as seen in the ACF and PACF plots and the stationarity test, thus, the integration part of the ARIMA process is zero, and the time series of log returns of carbon emission futures represents an MA process. An MA(2) was determined as the best model among ARMA(p,q) models. However, the prediction is quite poor due to the volatility of actual log returns of carbon emission futures.

Due to the presence of asymmetries within the log returns of carbon emission futures distribution, ARMA-exponential GARCH(p,q) models were investigated. MA(2)-EGARCH(2,2) as the variance model was found to have a great prediction of the volatility in both training data during 2017-2022 and testing data in 2023.

We plot the Autocorrelation Function (ACF) and Partial Autocorrelation Function (PACF) for the Log Returns and use it to determine the orders of the AR and MA processes respectively.

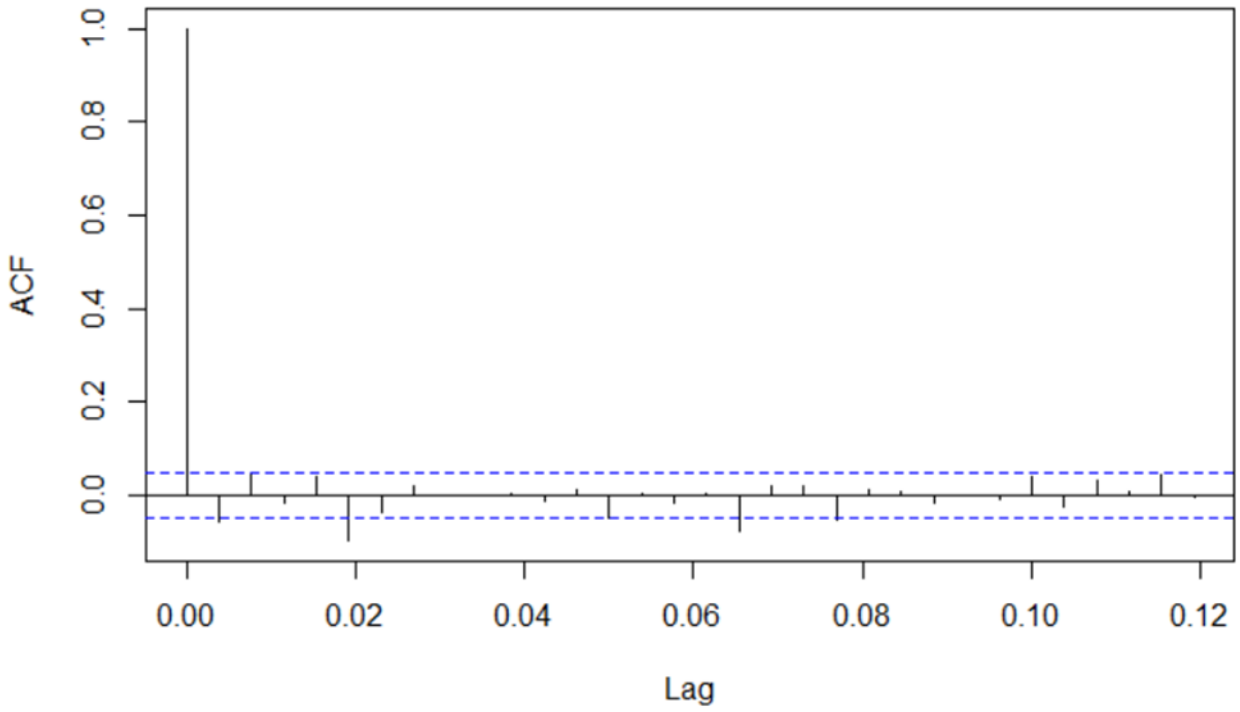

Figure 20. ACF of the log returns of carbon emission futures during 2017-2022

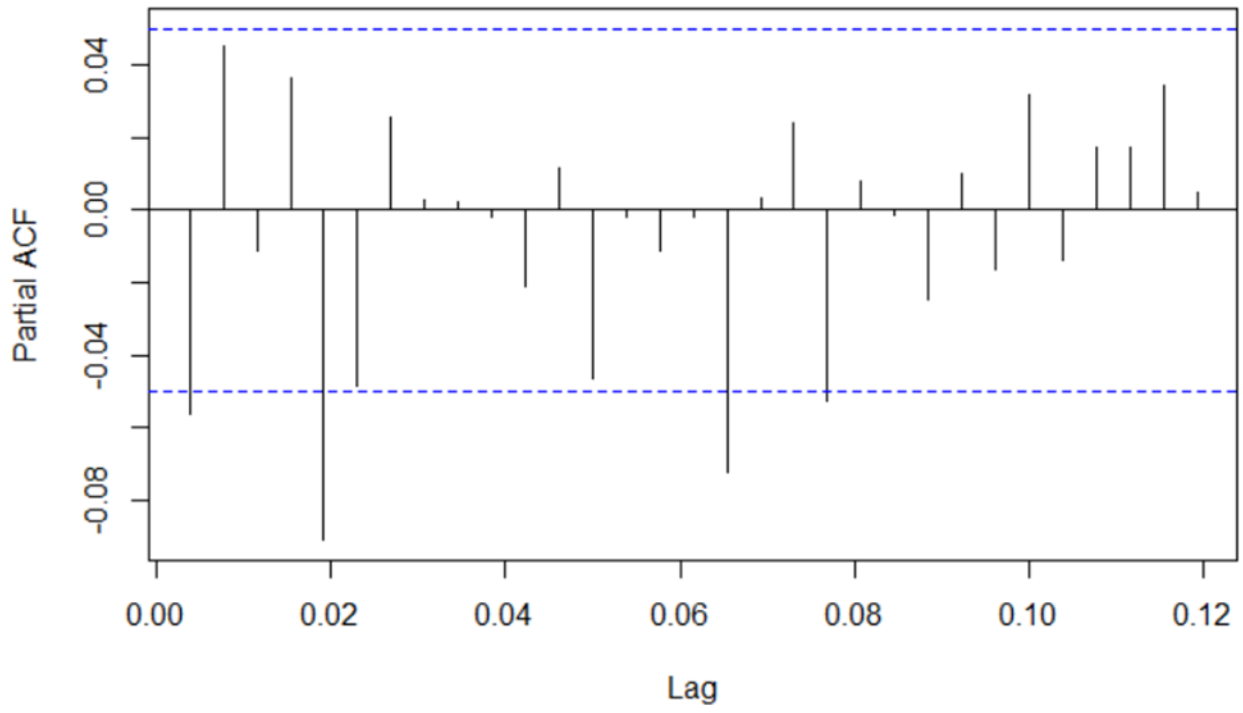

Figure 21. PACF of the log returns of carbon emission futures during 2017-2022

To check model fitting and diagnostics, the log returns time series was split into training and testing data where the training data was from 2017 to 2022. Test for stationarity is conducted using the Augmented Dickey-Fuller unit root test and visualizing autocorrelation (ACF) and partial

autocorrelation (PACF) plots. From the plots, we can see that the ACF has a significant spike at lag one, with none being significant after lag one. This implies that the series has an MA order.

```
        Augmented Dickey-Fuller Test

data:  lrpre
Dickey-Fuller = -11.891, Lag order = 11, p-value = 0.01
alternative hypothesis: stationary
```

Figure 22. ACF of the log returns of carbon emission futures during 2017-2022

The p-value resulting from the ADF test has to be less than 0.05 for a time series to be stationary. Since the p-value of the ADF test is 0.01 which is less than 0.05, we reject the Ho that the time series is non-stationary. Thus we conclude that the time series is a stationary process. Figure 4 of log returns confirms that the log return of carbon emission futures is a stationary process in the training data. PACF plot on the log returns shows that there might be some moving average (MA) lags.

5.3.1 ARIMA ANALYSIS

Since we inferred that an ARMA or ARIMA model would be a moving average (MA) model as the graphs displays its characteristics. Nevertheless, other techniques that could be useful to determine the right orders is to construct a matrix of models (with orders up to 2x2: 2 for AR and 2 for MA, and MA with orders from 0-5) and we choose the pair with the lowest Akaike information criterion (AIC) score.

Table 2: AIC values for estimated ARIMA(p,0,q)

	0	**1**	**2**
0	-6530.641	-6533.16	-6534.399
1	-6533.16	-6530.413	-6532.249
2	-6534.399	-6535.745	-6533.782

Table 3: AIC values for estimated MA(q)

q	**AIC**
1	-6533.16
2	-6534.399
3	-6532.417
4	-6532.169
5	-6546.551

Table 4: Coefficient tests for candidate models ARMA(2,1) and MA(2), MA(5)

```
z test of coefficients:

            Estimate Std. Error z value Pr(>|z|)
ar1       -0.7711294  0.2537710 -3.0387 0.002376 **
ar2        0.0037502  0.0394624  0.0950 0.924290
ma1        0.7203730  0.2523254  2.8549 0.004305 **
intercept  0.0016098  0.0007194  2.2378 0.025236 *
---
Signif. codes:  0 ‘***’ 0.001 ‘**’ 0.01 ‘*’ 0.05 ‘.’ 0.1 ‘ ’ 1


z test of coefficients:

             Estimate  Std. Error z value Pr(>|z|)
ma1       -0.05351346  0.02553505 -2.0957  0.03611 *
ma2        0.04498871  0.02492266  1.8051  0.07105 .
intercept  0.00161695  0.00073351  2.2044  0.02750 *
---
Signif. codes:  0 ‘***’ 0.001 ‘**’ 0.01 ‘*’ 0.05 ‘.’ 0.1 ‘ ’ 1


z test of coefficients:

            Estimate Std. Error z value  Pr(>|z|)
ma1       -0.0571055  0.0254282 -2.2458   0.02472 *
ma2        0.0518367  0.0256088  2.0242   0.04295 *
ma3       -0.0139262  0.0265474 -0.5246   0.59988
ma4        0.0404435  0.0260753  1.5510   0.12090
ma5       -0.1051579  0.0258203 -4.0727 4.648e-05 ***
intercept  0.0016237  0.0006741  2.4087   0.01601 *
---
Signif. codes:  0 ‘***’ 0.001 ‘**’ 0.01 ‘*’ 0.05 ‘.’ 0.1 ‘ ’ 1
```

Table 5. ACF of the log returns of carbon emission futures during 2017-2022

Tables 3-5 above shows the output of ARIMA models with orders p and q The minimum AIC value is -6546.551 for MA(5) model. However, the coefficient test shows that MA lags at 3 and 4 are not statistically significant. An estimation of the model can be seen above in table 5. Therefore, to be consistent with the PACF plot on the log returns which shows that there might be some moving average (MA) lags, we should use MA(2) model with both significant lags (instead of ARMA(2,1) or MA(5)).

MA(2) Model:

$$Y_t = \beta_0 + \epsilon_t + \theta_1 \epsilon_{t-1} + \theta_2 \epsilon_{t-2}$$

where

$$\epsilon_t \sim \text{WN}(0, \sigma^2)$$

From the estimation, we have:

$$Y_t = 0.016 + \epsilon_t - 0.0535 \epsilon_{t-1} + 0.045 \epsilon_{t-2}$$

We plot the residuals from the MA(2) model. The results are summarized below:

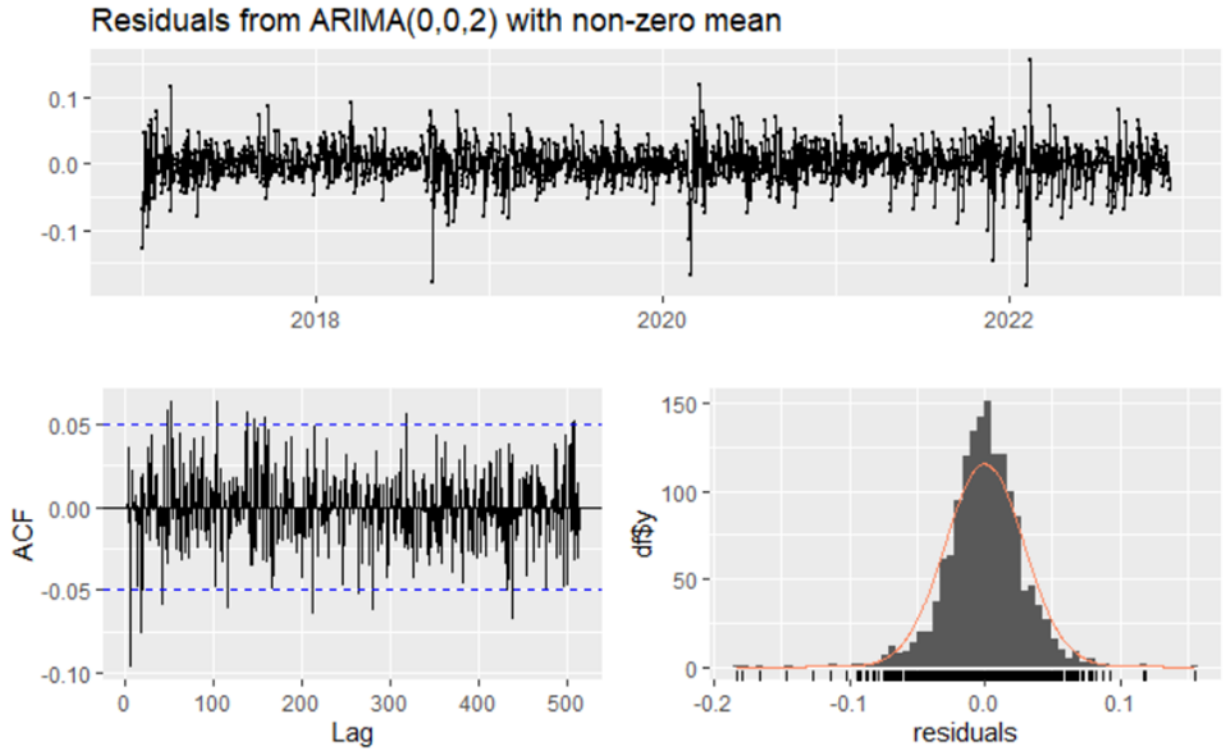

Figure 23 Residual analysis of log returns model MA(2).

```
        Ljung-Box test

data:  Residuals from ARIMA(0,0,2) with non-zero mean
Q* = 312.15, df = 306, p-value = 0.3921

Model df: 3.   Total lags used: 309
```

Figure 24 Ljung-Box test for residuals from MA(2).

The residual of the model MA(2) is shown in Figure 7 above. It can be observed that residuals have a mean value of zero but display a non-constant spread, especially during 2017-2022.

Figure 25 below shows the prediction for the period of 2017- 2022 to validate the model MA(2) and the forecast for 2023. The predicted values can be seen in orange, compared to the actual values in green. It is clear from **Figure 25** that the prediction is not good enough since it cannot capture the volatility of the data on daily log returns of carbon emission futures. Due to the presence of a non-constant spread, the volatility of the time series should be investigated using GARCH analysis as it is the most important factor for predicting the volatility of log returns of carbon emission futures.

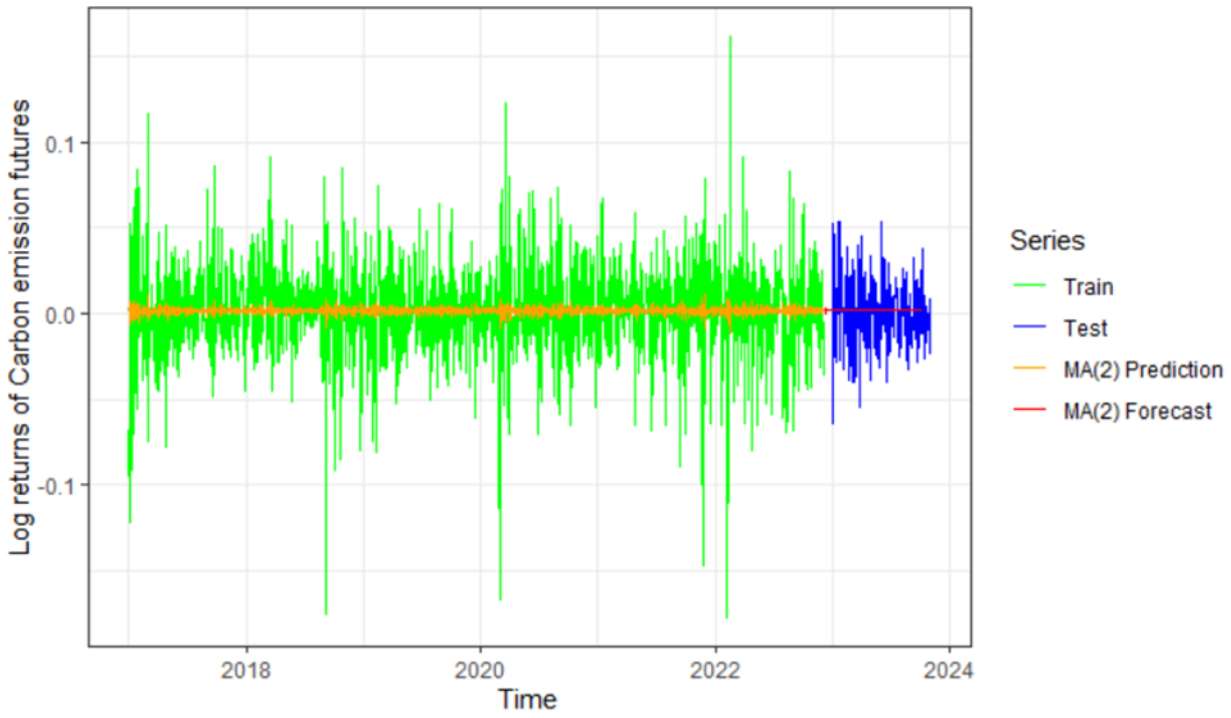

Figure 25 Time Series Plot for log returns of carbon emission futures and its prediction and forecasts during 2017-2023

5.3.2 EGARCH ANALYSIS

The exponential GARCH (eGARCH) variance model is capable to capture asymmetries within the volatility shocks. We have concluded MA(2) process models the data well. Now we try to find the order of the EGARCH model and estimate the model parameters.

$$Y_t = \beta_0 + u_t + \theta_1 u_{t-1} + \theta_2 u_{t-2}$$

$$u_t = \sigma_t \epsilon_t$$

$$\ln(\sigma_t^2) = \omega + \sum_{j=1}^{q} \left(\alpha_j \varepsilon_{t-j}^2 + \gamma(\varepsilon_{t-j} - E|\varepsilon_{t-j}|)\right) + \sum_{i=1}^{p} \beta_i \ln(\sigma_{t-i}^2)$$

where Y_t is the log returns of carbon emission futures ϵ_t is the shock and ϵ_t WN(0,σ_t^2) σ_t^2 is the volatility ω , α , β are coefficients that will be estimated.
Compare EGARCH models to determine which model with the best AIC newline Conducting many EGARCH models to fit out, the conclusion is that MA(2)-EGARCH(2,2) was the best as it had the lowest AIC value of and all the coefficients are statistically significant, as shown in Table 5 below.

Table 4: AIC values for estimated MA(2)-EGARCH(p,q)

p, q	AIC
1,1	-6796.329
1,2	-6796.542
2,1	-6797.02
2,2	-6821.919

Optimal Parameters

	Estimate	Std. Error	t value	Pr(>|t|)
mu	0.002205	0.000085	25.859	0
ma1	-0.062756	0.003027	-20.732	0
ma2	0.032815	0.001283	25.568	0
omega	-1.142052	0.000358	-3186.027	0
alpha1	-0.015810	0.000009	-1782.647	0
alpha2	-0.017153	0.000023	-747.051	0
beta1	-0.072046	0.000001	-51012.409	0
beta2	0.914129	0.000013	70489.438	0
gamma1	0.200231	0.000075	2683.372	0
gamma2	0.139752	0.000105	1330.052	0
skew	0.968612	0.032533	29.773	0
shape	5.819244	0.220290	26.416	0

Table 5: Estimation Results of MA(2)-EGARCH(2,2)

The MA(2) + EGARCH(2,2) fit also provides with significant coefficients, no correlation within standardized residuals, no correlation within standardized squared residuals and all ARCH effects are properly captured.

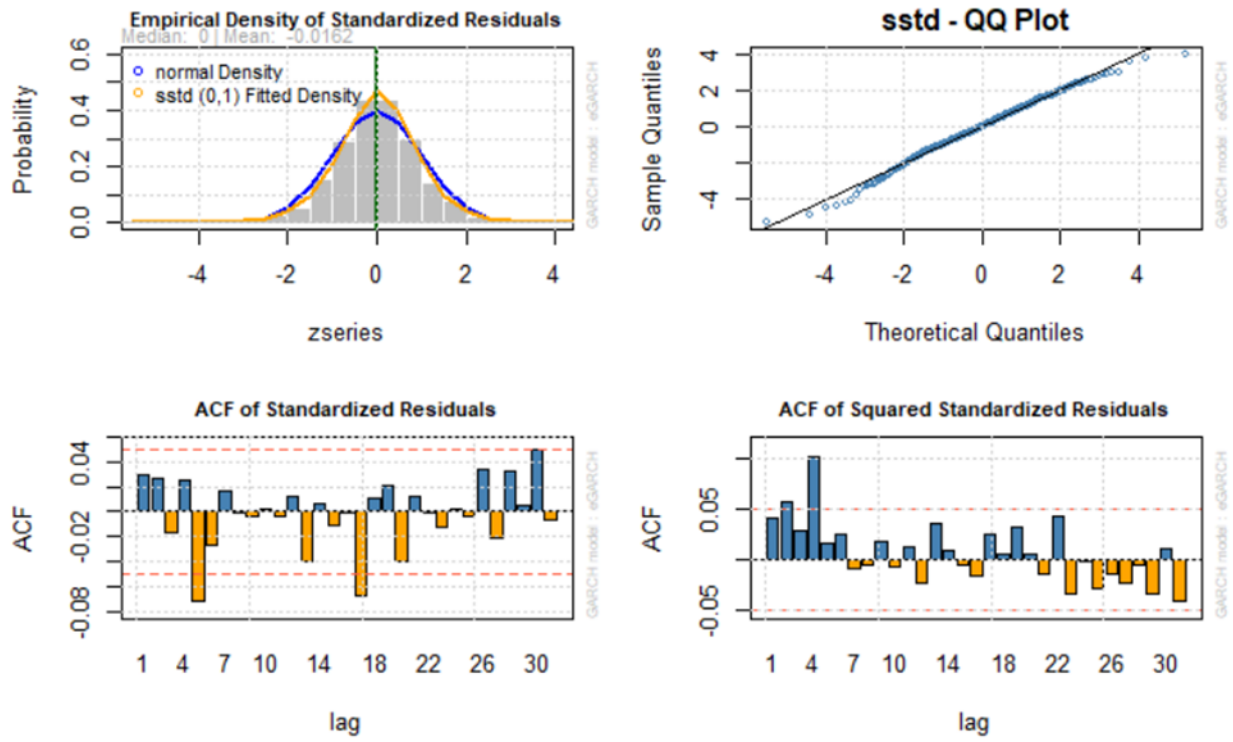

Figure 26 Residual Plots for EGARCH models

```
Weighted Ljung-Box Test on Standardized Residuals
-----------------------------------
                        statistic p-value
Lag[1]                      1.338 0.24745

Weighted Ljung-Box Test on Standardized Squared Residuals
-----------------------------------
                         statistic   p-value
Lag[1]                       2.519 0.1124475

Weighted ARCH LM Tests
-----------------------------------
            Statistic Shape Scale P-Value
ARCH Lag[5]    0.3354 0.500 2.000  0.5625
ARCH Lag[7]    1.2044 1.473 1.746  0.7008
ARCH Lag[9]    1.5323 2.402 1.619  0.8463
```

Figure 27 Ljung- Box for EGARCH residuals

Using the MA(2) + EGARCH(2,2) coefficients, we have the results:

$$Y_t = 0.016 + u_t - 0.0535u_{t-1} + 0.045u_{t-2}$$
$$u_t = \sigma_t \varepsilon_t$$

$$\ln(\sigma_t^2) = -1.142 - 0.016\varepsilon_{t-1}^2 - 0.017\varepsilon_{t-2}^2 + 0.2(\varepsilon_{t-1} - E(\varepsilon_{t-1})) + 0.14(\varepsilon_{t-2} - E(\varepsilon_{t-2})) - 0.072\ln(\sigma_{t-1}^2) + 0.914\ln(\sigma_{t-2}^2)$$

A volatility prediction made between the period 2017-2022 to validate the MA(2)-EGARCH(2,2) model indicates a better fit to the actual volatility than the model MA(2) as seen below in **Figure 28**. The actual values are presented in grey color while the predicted values are represented in green color. **Figure 29** shows that both the prediction within 2017-2022 (grey) and the forecasted values in 2023 (green) are matched with the actual values of log returns of carbon emission futures in blue color.

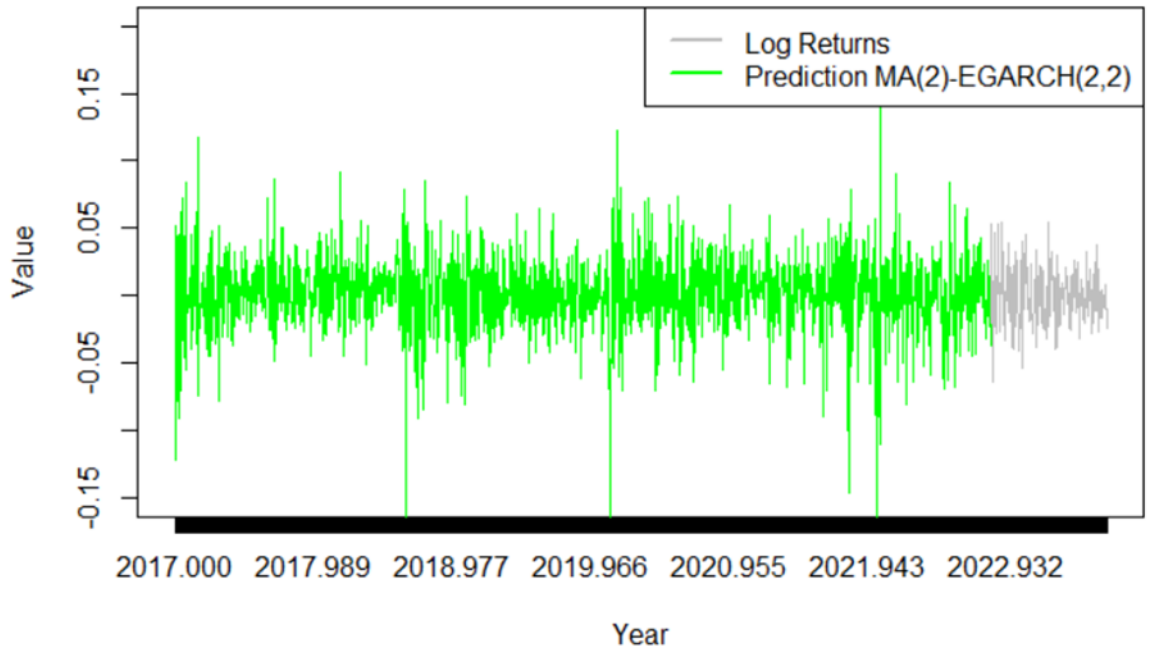

Figure 28: Time Series Plot for log returns of carbon emission futures and its prediction during 2017-2022 using MA(2)-EGARCH(2,2)
(Note: the prediction is right on top of the actual values during 2017-2022, the actual values in 2023 are in grey)

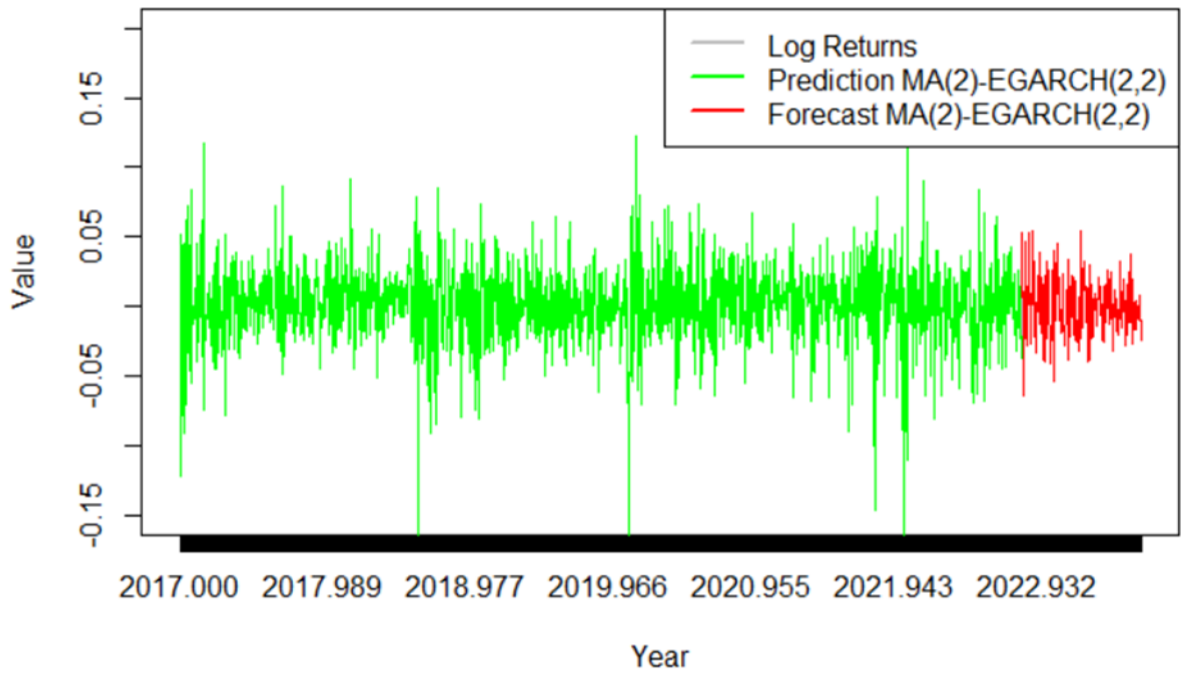

Figure 29: Time Series Plot for log returns of carbon emission futures and its prediction and forecasts during 2017-2023 using MA(2)-EGARCH(2,2)

6 Conclusion

In conclusion, our examination of EU carbon emissions futures unveiled valuable insights into both short-term dynamics and long-term patterns. A time series econometrics model is developed to predict values of log returns of carbon emission futures using data during. An application of an modeling technique (ARMA - EGARCH) is used be to analyze the moving average and volatility of the time series and the best model MA(2)-EGARCH(2,2) was found the best fitted model in predicting carbon emission futures for the period of most recent years. In studying the dynamics of the EU ETS market, we discover interplay between EU carbon emissions futures and Tesla stock prices revealed a noteworthy relationship between environmental and financial markets. The share prices of green tech stocks such as Tesla have a strong influence on carbon emissions futures and can even be used to predict the latter. At times, they are even more influential than traditional financial indices, which is worth exploring further. In addition, we uncovered the signs of long-term instability in the dataset, specifically involving stochastic trends and very weak seasonal patterns, emphasizing the importance of constantly adapting to changing market conditions. These changes also parallel the recent major green swan event (i.e., COVID-19), which may also impede forecasting. This research contributes to learning about financial indices and provides insights for investors, policymakers, and market participants. As we delve into the broader context of climate finance, these findings lay a foundation for strategic planning and understanding market dynamics.

References

[1] "EU Emissions Trading System (EU ETS)." *Climate Action*, climate.ec.europa.eu/eu-action/eu-emissions-trading-system-eu-ets_en. Accessed 15 Dec. 2023.

[2] "Carbon Emissions Futures Historical Prices." *Investing.com*, www.investing.com/commodities/carbon-emissions-historical-data. Accessed 10 Dec. 2023.

[3] "DJ Oil & Gas Historical Rates (DJUSEN)." *Investing.com*, www.investing.com/indices/dj-oil---gas-historical-data. Accessed 10 Dec. 2023.

[4] M. E. H. Arouri, F. Jawadi, and D. K. Nguyen. Nonlinearities in carbon spot-futures price relationships during phase ii of the eu ets. *Economic Modelling*, 29(3):884–892, 2012.

[5] P. Bolton, M. Luiz, A. Pereira, D. Silva, F. Samama, and R. Svartzman. *The green swan Central banking and financial stability in the age of climate change*. 01 2020.

[6] G. Daugherty. "Carbon Markets: What They Are and How They Work." *Investopedia*, https://www.investopedia.com/carbon-markets-7972128. Accessed 15 Dec. 2023.

[7] Y. Huang, X. Dai, Q. Wang, and D. Zhou. A hybrid model for carbon price forecastingusing garch and long short-term memory network. *Applied Energy*, 285:116485, 2021.

[8] W. Li and C. Lu. The research on setting a unified interval of carbon price benchmark in the national carbon trading market of china. *Applied Energy*, 155:728–739, 2015.

[9] H. Sharma. Carbon pricing - markets, taxes or regulation? *Green Fiscal Policy Network*, 14 May 2021.

[10] B. Zhu and Y. Wei. Carbon price forecasting with a novel hybrid arima and least squares support vector machines methodology. *Omega*, 41(3):517–524, 2013.